Macromolecules

NOTE

pubs.acs.org/Macromolecules

Polypeptide-Based Organogelators: Effects of Secondary Structure

Florian Hermes,[†,§] Katharina Otte,[†] Jessica Brandt,[†] Marlies Gräwert,[†] Hans G. Börner,[‡] and Helmut Schlaad*[,†]

[†]Max Planck Institute of Colloids and Interfaces, Research Campus Golm, 14424 Potsdam, Germany

[‡]Humboldt-Universität zu Berlin, Department of Chemistry, Laboratory of Organic Synthesis of Functional Systems, Brook-Taylor-Str. 2, 12489 Berlin, Germany

INTRODUCTION

Bioinspired block copolymers comprising synthetic polymer and polypeptide block segments, also referred to as polypeptide hybrid copolymers, bioconjugates, or "macromolecular chimeras",[1] have been in the focus of polymer science for now more than four decades.[2] Polypeptide block polymers are readily available through ring-opening polymerization of amino acid *N*-carboxyanhydrides (NCA, Leuchs' anhydrides)[3] using amino-functionalized macroinitiators, as pioneered by Gallot and co-workers.[4,5] More sophisticated and effective methods of NCA polymerization have later been developed by Deming and others, enabling the synthesis of well-defined polypeptides and polypeptide hybrid copolymers in larger amounts.[6,7] Besides, automated solid-phase supported peptide synthesis (SPPS)[8] has emerged as an established and robust synthesis tool to make peptide−polymer conjugates with monodisperse, monomer sequence-defined peptide segments.[9−12]

So far, amino acid sequences of peptides in bioconjugates have been intensively altered to study the impact of hydrophilic/hydrophobic pattern as well as the order and type of functional groups on interaction capabilities or propensities to fold into secondary or quaternary structures.[13] Although the importance of secondary structure on self-assembly phenomena was often highlighted, the separation of secondary structure effects from other driving forces that determine self-assembly in such polar block copolymer systems remains difficult. Only few attempts have been made to directly evaluate these effects. This, however, would be interesting for understanding soft matter assembly processes, for instance organo- or hydrogelation. Altering the stereoisomers of peptide segments within bioconjugates without changing the amino acid sequence might enable the decoupling of secondary structure effects from chemical composition and hence provides insight into self-assembly processes.

Initial important contributions in this field were made by Deming and co-workers.[14−16] Block extension of a poly(L-lysine)$_{180}$ (the subscript denoting the average number of repeat units) by copolymerization a mixture of D- and L-leucine-NCAs yielded a poly(L-lysine)$_{180}$-*block*-poly(DL-leucine)$_{40}$ with a statistic stereosequence in the polyleucine block. Rheology revealed a significantly increased critical gelation concentration and strongly reduced gel strength if this polymer was compared to the homo stereoisomeric compound poly(L-lysine)$_{180}$-*block*-poly(L-leucine)$_{40}$.

Jeong et al.[17,18] studied aqueous solutions of L/DL-polyalanine-based block copolymers according to reverse thermal gelation behavior and ability to form fibrous nanostructures. The L-isomer with a preassembled β-sheet secondary structure was found to facilitate the sol−gel transition and nanofiber formation rather than the DL-isomer with random coil structure.

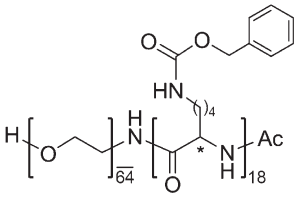

Sample	(ZLys)$_{18}$ Stereosequence	(ZLys)$_{18}$ Conformation
1 PEO$_{64}$-*b*-(ZLys)$_{18}^{coil}$	DDLLLDDLDLLLDLLDLD	random coil
2 PEO$_{64}$-*b*-(ZLys)$_{18}^{sheet}$	LLLLLLLDDDDLLLLLLL	β-sheet
3 PEO$_{64}$-*b*-(ZLys)$_{18}^{helix}$	LLLLLLLLLLLLLLLLLL	α-helix

Figure 1. Molecular structure of poly(ethylene oxide)-(Z-lysine)$_{18}$ conjugates **1**−**3**.

Here, we address the phenomenon of secondary structure effects on bioconjugate self-assembly in a systematic manner. Three bioconjugate samples of poly(ethylene oxide)$_{64}$-*block*-[(N^{ε}-benzyloxycarbonyl)lysine]$_{18}$ (PEO$_{64}$-ZLys$_{18}$) comprising monodisperse peptide segments of predefined stereosequences and thus secondary structures (Figure 1) were synthesized by SPPS and examined according to their ability to gelate tetrahydrofuran (THF) at room temperature.

EXPERIMENTAL PART

Materials. The resin TentaGel Wang PAP (4-hydroxymethyl phenoxymethyl (Wang) polystyrene attached poly(ethylene oxide); loading 0.20 mmol/g) was synthesized in collaboration with Rapp Polymere (Tübingen, Germany) as previously reported.[19] Fmoc-L-Lys(Z)OH and Fmoc-D-Lys(Z)OH (Lys = lysine, Fmoc = fluorenylmethoxycarbonyl, Z = benzyloxycarbonyl) and 2-(1*H*-benzotriazole-1-yl)-1,1,3,3-tetramethyluronium hexafluorophosphate (HBTU) were purchased from Iris Biotech and used as received. *N*,*N*-Diisopropylethylamine (DIPEA) and trifluoroacetic acid (TFA, 99.5% for biochemistry) were received from Acros Organics and distilled. Piperidine (99+% extra pure; Acros

Received: May 31, 2011
Revised: August 12, 2011
Published: August 26, 2011

Organics) was used as received. *N*-Methyl-2-pyrrolidone (NMP, peptide grade; Iris Biotech GmbH, Germany) was freshly filtered through aluminum oxide and silica gel. Dichloromethane (DCM, peptide grade; Iris Biotech) was stirred over calcium hydride and distilled. THF, diethyl ether, and benzene from Sigma-Aldrich were used as received.

General Procedure (Synthesis of PEO−Peptide Conjugates). The synthesis was performed in a 0.1 mmol scale, using a fully automated ABI 433a peptide synthesizer (Applied Biosystems, Darmstadt, Germany) and TentaGel Wang PAP resin as solid support (0.20 mmol/g). Peptide synthesis was performed in NMP as the solvent following modified ABI-Fastmoc protocols. Amino acid coupling was facilitated using HBTU/DIPEA. L-Amino acid derivatives were coupled with single coupling procedures and extended coupling times (75 min) using 10-fold amino acid excess. The coupling of the D-amino acid derivatives followed single coupling procedures with 5-fold amino acid excess but extended 110 min coupling times. After final Fmoc-group removal, the N-terminal amino group was acetylated. The Z-protected bioconjugates were liberated by treatment of the resin with 30% TFA in DCM for 30 min. The bioconjugates were isolated by diethyl ether precipitation, reprecipitation, followed by lyophilization from benzene.

Analytical Instrumentation and Methods. ^{1}H NMR measurements were carried out at room temperature or +100 °C using a Bruker DPX-400 spectrometer operating at 400.1 MHz. DMF-d_7 was used as solvent; signals were referenced to the signal of solvent at δ = 8.0 ppm. Fourier-transform infrared (FT-IR) spectra were recorded on a BioRad 6000 FT-IR spectrometer. Samples were measured at room temperature in the solid state using a single reflection diamond ATR. Circular dichroism (CD) spectra were recorded on a Jasco J-715 spectrometer at room temperature. Polymer solutions (0.1−1 mg/mL in THF) were measured in quartz cuvettes of 1 mm path length. Liquid chromatography (LC) (size-exclusion chromatography, SEC) with simultaneous UV and RI detection was performed (i) in THF at 25 °C using a column set of two 300 × 8 mm^2 MZ-SDplus (spherical polystyrene particles with an average diameter of 5 μm) columns with porosities of 10^3 and 10^5 Å or (ii) in *N*-methyl-2-pyrrolidone (NMP + 0.5 wt % LiBr) at +70 °C using a column set of two 300 × 8 mm^2 PSS-GRAM (spherical polyester particles with an average diameter of 7 μm) columns with porosities of 10^2 and 10^3 Å, respectively. Solutions containing ~0.15 wt % polymer were filtered through 0.45 μm filters; the injected volume was 100 μL. Calibration was done with poly(ethylene oxide) standards (Polymer Standards Service PSS, Mainz, Germany). Viscosity measurements were performed with an automated micro viscometer AMVn (Anton Paar) applying the falling ball method. Depending on the sample viscosity, a glass capillary with a diameter of 1.6 or 1.8 mm and a ball with a diameter of 1.5 mm were used. Scanning force microscopy (SFM) measurements were performed on a Nanoscope Multimode IIIa microscope (Digital Instruments, Santa Barbara, CA) using silicon cantilevers with k = 42 N/m (Nanoworld, Switzerland). Surfaces were scanned at room temperature in tapping mode at a resonance frequency of 200−300 kHz. Samples were spin-coated at 2000 rpm onto UV/ozone-cleaned silicon wafers.

RESULTS AND DISCUSSION

Three poly(ethylene oxide)$_{\overline{x}}$-*block*-(Z-lysine)$_y$ (PEO−ZLys) conjugates with predefined stereoisomeric 18-mer peptide segments (see Figure 1) were prepared by Fmoc solid-phase peptide synthesis.[20] Amino acids, Fmoc-L-Lys(Z)-OH and Fmoc-D-Lys-(Z)-OH, were coupled on a Tentagel-Wang PAP resin, which was preloaded with an amino-functional PEO (number-average degree of polymerization, $\overline{x}$ = 64, polydispersity index, PDI = 1.08, as determined by SEC). The coupling of amino acids was accomplished applying automated FastMoc protocols, using Fmoc-Lys(Z)-OH at 10-fold (L enantiomer) or 5-fold excess

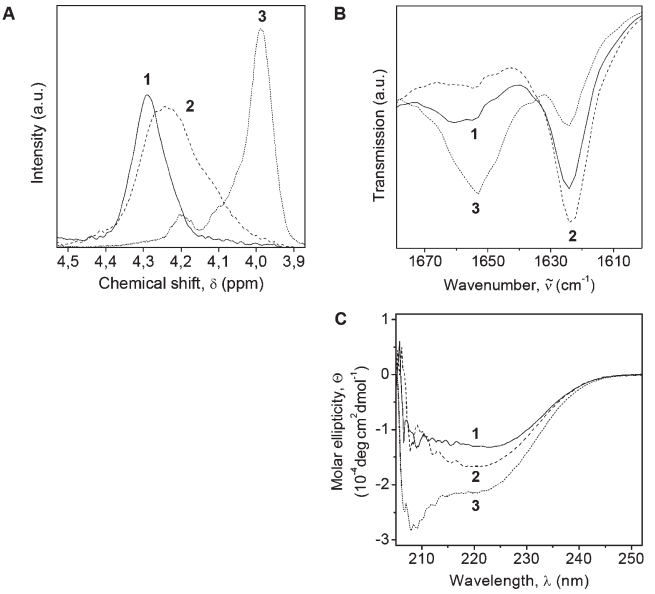

Figure 2. (A) ^{1}H NMR spectra (400.1 MHz, DMF-d_7) of the α-CH protons, (B) FT-IR spectra (ATR, solid state) of the amide I vibrations, and (C) CD spectra (1 mg/mL, THF) of samples **1**−**3**.

(D enantiomer). The terminal amino group of the peptide was finally acetylated before the bioconjugate was cleaved off from the resin by treatment with TFA. The PEO−peptide conjugates were isolated by precipitation into DCM/diethyl ether and freeze-drying from benzene.

Quantitative Fmoc monitoring via UV spectroscopy suggested a clean assembly of the peptide segments. ^{1}H NMR spectroscopic analyses (DMF-d_7, 100 °C) (data not shown) confirmed this by indicating that the products had the expected molecular composition as depicted in Figure 1. The molar ratios of ZLys/EO, as determined by ^{1}H NMR spectroscopy considering the integral intensities of the signals at $\delta \sim$ 5.1 ppm (ZLys, Bzl-CH$_2$, $y \times$ 2H) and 3.6 ppm (EO, OCH$_2$, $\overline{x} \times$ 4H), were found to be in the range of 0.26−0.27 and thus meet the expected value of 0.28 (ZLys/EO 18/64) very well within the experimental error. The weight fraction of ZLys is w_{ZLys} = 0.62. The estimated diameter of a randomly coiled PEO$_{64}$ chain is $d = 2R_g \approx$ 2.3 nm, and the contour lengths of the ZLys segments are $l_c \approx 18 \times 0.36$ nm = 6.5 nm (*all-trans* conformation or β-sheet) and 18 × 0.17 nm = 3.1 nm (α-helix).[21]

The stereosequences of ZLys segments of samples **1**−**3** were designed in a way that the peptides should adopt random coil (**1**), β-sheet (**2**), and α-helix (**3**) conformations or secondary structures (Figure 1). The first sequence is a random series of 8 D-ZLys and 10 L-ZLys units, the second is a stereoblock sequence comprising two blocks of 7 L-ZLys and one block of 4 D-ZLys, and the third is a homochiral block of 18 L-ZLys.

The true secondary structure of samples **1**−**3** was characterized by means of ^{1}H NMR (DMF-d_7, rt) and FT-IR spectroscopy (solid state, rt).[22,23] The α-CH spectrum ($\delta \sim$ 3.9−4.4 ppm) of **1**−**3** (Figure 2A) is most sensitive to the secondary structure of the peptide block. Based on the peak assignments reported in literature for poly(γ-benzyl glutamate)s in DMF solution,[22] the ZLys segment of **1** should have a predominant random coil structure (absorption centered at about 4.3 ppm) and that of **3** a helical structure (4.0 ppm), as expected. The α-CH spectrum of sample **2** is distinctively different from the other spectra,

exhibiting a very broad multiple signal at 4.0−4.4 ppm, which could not be assigned yet. However, the amide I infrared absorption bands (Figure 2B, $\tilde{\nu}$ = 1624 cm^{-1}) suggested that the ZLys segment of sample **2** adopts a β-sheet conformation.[23] FT-IR spectroscopy confirms the predominant α-helical structure of sample **3** ($\tilde{\nu}$ = 1655 cm^{-1}) but also reveals some minor amount of β-sheet. Sample **1** should, according to FT-IR, contain β-sheet and random coil ($\tilde{\nu}$ = 1660 cm^{-1}) fractions. NMR and FT-IR results are, for whatever reason, not in perfect agreement but essentially confirm the expected secondary structures of samples **1**−**3** (Figure 1). Circular dichroism (CD) spectroscopic analyses of THF solutions of **1**−**3**, however, provide little additional or vague insights in the secondary structures (Figure 2C). Very similar CD spectra were recorded for 0.1 and 1 mg/mL polymer solutions.

Samples **1**−**3** were further analyzed by liquid chromatography (LC), using either THF as mobile phase and polystyrene as stationary phase (MZ-SDplus) (Figure 3A) or NMP (+ 0.5 wt % LiBr) as mobile phase and polyester as stationary phase (PSS-GRAM) (Figure 3B). Despite the identical chemical compositions and molecular weights, all three samples display different chromatograms in THF depending on the secondary structure. Only sample **1** with a random coil conformation elutes faster than the corresponding PEO precursor and thus seems to elute in the size exclusion mode. The chromatograms of samples **2** and **3**, on the other hand, display multimodal peaks shifted to larger elution volumes, indicating adsorption of the peptide sheets or helices onto the hydrophobic polystyrene stationary phase. Adsorption is especially pronounced for the β-sheet sample **2**. Quantitative analysis of the peak integral suggests that only about 20% of the injected mass of sample **2** could be recovered.

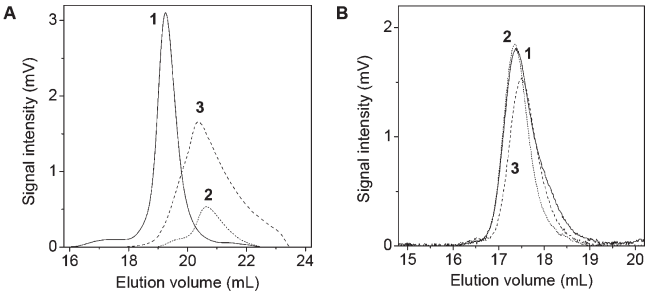

Figure 3. Liquid chromatograms of samples **1**−**3** using (A) THF as mobile phase and polystyrene as stationary phase and (B) NMP + 0.5 wt % LiBr as mobile phase and polyester as stationary phase (T = 70 °C).

The differences in elution behavior may vanish when more polar mobile (NMP/LiBr) and stationary phases (PSS-GRAM) are used at elevated temperature (+70 °C). Then, as shown in Figure 3b, all samples **1**−**3** elute in the size exclusion mode and display very similar, not yet identical, chromatograms.

Samples **1**−**3** were then examined according to gelation of THF at room temperature using viscometry and scanning force microscopy (SFM); the minimum gelation concentration was determined by the inverted-tube method (ITM).

Sample **1** could be readily dissolved in THF at room temperature at 5 mg/mL (about 3× higher concentration as used for SEC analyses), whereas samples **2** and **3** had to be treated with heat or ultrasound to accomplish complete dissolution. Figure 4A shows the time-dependent evolution of the dynamic viscosity of these solutions at room temperature. The dynamic viscosity of sample **1** showing the random coil structure in THF remained constant over time, η = 0.52 mPa·s (THF: η = 0.48 mPa·s), indicating that the solution was stable without evidence of gelation. The dynamic viscosities of **2** and **3**, on the other hand, were increasing with time due to the slow formation of fibrils (see below), finally leading to gelation. Importantly, the increase of viscosity is much more pronounced for sample **2** as compared to **3**, suggesting that the bioconjugate exhibiting β-sheet secondary structure has a considerably higher tendency to form a gel than that with an

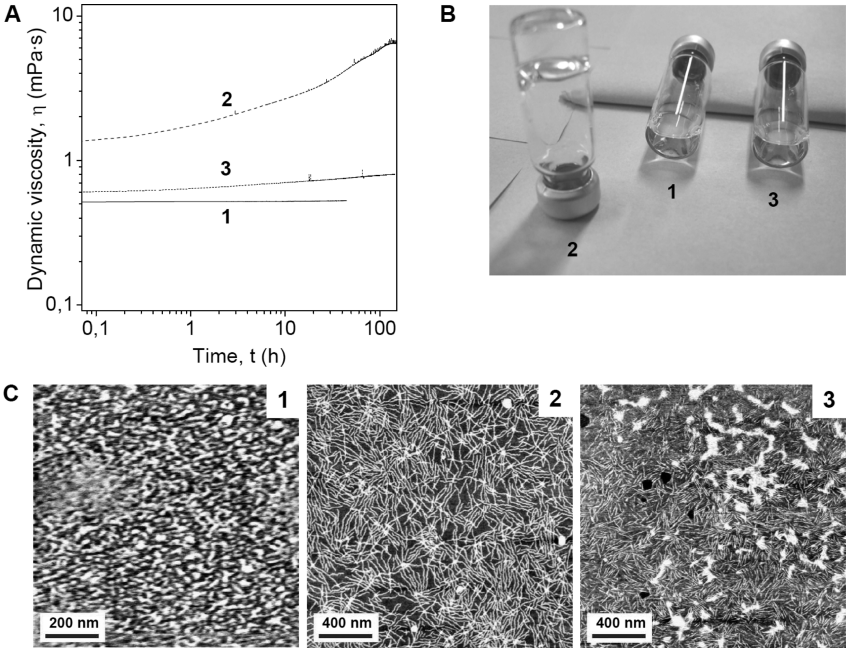

Figure 4. (A) Time-dependent evolution of the dynamic viscosity of THF solutions of **1**−**3** (5 mg/mL) at room temperature. (B) Photographs and (C) SFM height images (z-scale: 3 nm) of samples of **1**−**3** at 20 mg/mL in THF. For SFM imaging, original solutions were rapidly diluted 1:100 with THF and spin-coated onto silicon wafers.

dx.doi.org/10.1021/ma201232a |*Macromolecules* 2011, 44, 7489–7492

α-helical peptide conformation. The different gelation behaviors of samples **1**−**3** were also expressed by the minimum gelation concentrations as simply determined by ITM (Figure 4B). Solutions of **2** and **3** turned into self-supporting gels at minimum concentrations of 15 and 40 mg/mL, respectively; gelation of THF with **1** could not be observed.

The structures of **1**−**3** formed at 20 mg/mL in THF (**1** and **3** were liquids and **2** was a gel; Figure 4B) were visualized by scanning force microscopy (SFM; Figure 4C). Sample **1** showed a disordered film with features being 1 nm in height and 20−40 nm in diameter, supposedly originating from collapsed spherical micelles. (A compact sphere, having the same volume as a disk being 30 nm in diameter and 1 nm in height, measures ∼5.5 nm in radius, which is a rough estimation of the original size of micelles.) The images of **2** and **3** instead displayed nanofibrils (or nanoribbons). Evidently, the fibrils of the gelled sample **2** were considerably longer than those of the nongelled sample **3**. The fibrils of **2** were about 1 nm in height and 10−14 nm in width and thus meet the dimensions of β-sheet assemblies of congener PEO−peptide conjugates.[24] Considering the contour length of the polymer chains (see above), fibrillization seems to occur via antiparallel β-sheet formation which would theoretically lead to fibrils with estimated width of (2.3 + 6.5 + 2.3) nm = 11.1 nm. The fibrils formed by sample **3** were 6−10 nm in width. These dimensions can be explained by a structure of interdigitated α-helices, i.e., 2.3 nm + 3.1 nm + 2.3 nm = 7.7 nm, as has earlier been reported in the literature.[16,25−27] It is evident that the PEO−peptide molecules are oriented orthogonal to the fibril axis, which is distinctively a different case as for α-helical polypeptide homopolymers (where the helices are oriented parallel to the fibril axis and joined end to end).[28,29] Steric repulsion of the second block segment may be a good explanation for the observed packing and orientation of α-helices, but not for the directed assembly into fibrils.[16,25] In fact, many examples of (neutral) polymer−peptide conjugates are known to self-assemble into 2D sheetlike structures, i.e., vesicles, rather than 1D fibrillar structures.[30,31] The mechanism discriminating between the 1D and 2D self-assembly of α-helices is still not fully understood yet. One hypothesis relies on the directional 1D packing of dipolar α-helices in quadrupols—this, however, has to be proven by further studies.

CONCLUSION

Three poly(ethylene oxide)$_{\bar{x}}$-*block*-(Z-lysine)$_y$ (PEO-ZLys) conjugates with the same chemical composition comprising 18-mer peptide segments of predefined stereosequences and thus secondary structures (as analyzed by ^{1}H NMR, FT-IR, and CD spectroscopy) were studied according to their different solution behaviors and abilities to gel THF. The tendency for organogelation increases for the PEO−peptide conjugates in the order of the peptide segment to form random coil < α-helix < β-sheet. This was evidenced by time-dependent evolution of viscosity, minimum gelation concentrations (ITM), and morphologies of the solution/gel (SFM).

AUTHOR INFORMATION

Corresponding Author

*Fax +49.331.567.9502, e-mail schlaad@mpikg.mpg.de.

Present Addresses

§Evonik Industries AG Hanau, Germany.

ACKNOWLEDGMENT

Ines Below-Lutz, Antje Völkel, and Olaf Niemeyer are thanked for their contributions to this project. Markus Antonietti is thanked for fruitful and stimulating discussions. Financial support was given by the Max Planck Society and, as part of the EUROCORES Programme BIOSONS, by the German Research Foundation. H.G.B. acknowledges funding from the German Research Foundation (DFG, BO 1762/2-2&3).

REFERENCES

(1) Schlaad, H.; Antonietti, M. *Eur. Phys. J. E* **2003**, *10*, 17–23.
(2) Börner, H. G.; Schlaad, H. *Soft Matter* **2007**, *3*, 394–408.
(3) Leuchs, H. *Ber. Dtsch. Chem. Ges.* **1906**, *39*, 857–861.
(4) Perly, B.; Douy, A.; Gallot, B. *C. R. Acad. Sci., Ser. C* **1974**, *279*, 1109–1111.
(5) Gallot, B. *Prog. Polym. Sci.* **1996**, *21*, 1035–1088.
(6) Deming, T. J. *Nature* **1997**, *390*, 386–389.
(7) Deming, T. J. *Adv. Polym. Sci.* **2006**, *202*, 1–18.
(8) Merrifield, R. B. *J. Am. Chem. Soc.* **1963**, *85*, 2149–2154.
(9) Maynard, H. D.; Okada, S. Y.; Grubbs, R. H. *J. Am. Chem. Soc.* **2001**, *123*, 1275–1279.
(10) Hamley, I. W.; Ansari, A.; Castelletto, V.; Nuhn, H.; Rösler, A.; Klok, H. A. *Biomacromolecules* **2005**, *6*, 1310–1315.
(11) Lutz, J. F.; Börner, H. G. *Prog. Polym. Sci.* **2008**, *33*, 1–39.
(12) Canalle, L. A.; Lowik, D.; van Hest, J. C. M. *Chem. Soc. Rev.* **2010**, *39*, 329–353.
(13) Börner, H. G. *Prog. Polym. Sci.* **2009**, *34*, 811–851.
(14) Nowak, A. P.; Breedveld, V.; Pakstis, L.; Ozbas, B.; Pine, D. J.; Pochan, D.; Deming, T. J. *Nature* **2002**, *417*, 424–428.
(15) Breedveld, V.; Nowak, A. P.; Sato, J.; Deming, T. J.; Pine, D. J. *Macromolecules* **2004**, *37*, 3943–3953.
(16) Deming, T. J. *Soft Matter* **2005**, *1*, 28–35.
(17) Choi, Y. Y.; Joo, M. K.; Sohn, Y. S.; Jeong, B. *Soft Matter* **2008**, *4*, 2383–2387.
(18) Oh, H. J.; Joo, M. K.; Sohn, Y. S.; Jeong, B. *Macromolecules* **2008**, *41*, 8204–8209.
(19) Hartmann, L.; Krause, E.; Antonietti, M.; Börner, H. G. *Biomacromolecules* **2006**, *7*, 1239–1244.
(20) Hentschel, J.; Krause, E.; Börner, H. G. *J. Am. Chem. Soc.* **2006**, *128*, 7722–7723.
(21) Losik, M.; Kubowicz, S.; Smarsly, B.; Schlaad, H. *Eur. Phys. J. E* **2004**, *15*, 407–411.
(22) Paolillo, L.; Temussi, P.; Trivellone, E.; Bradbury, E. M.; Crane-Robinson, C. *Macromolecules* **1973**, *6*, 831–838.
(23) Miyazawa, T.; Blout, E. R. *J. Am. Chem. Soc.* **1961**, *83*, 712–719.
(24) Börner, H. G.; Smarsly, B.; Hentschel, J.; Rank, A.; Schubert, R.; Geng, Y.; Discher, D. E.; Hellweg, T.; Brandt, A. *Macromolecules* **2008**, *41*, 1430–1437.
(25) Kim, K. T.; Park, C.; Vandermeulen, G. W. M.; Rider, D. A.; Kim, C.; Winnik, M. A.; Manners, I. *Angew. Chem., Int. Ed.* **2005**, *44*, 7964–7968.
(26) Naik, S. S.; Savin, D. A. *Macromolecules* **2009**, *42*, 7114–7121.
(27) Schlaad, H.; Kukula, H.; Smarsly, B.; Antonietti, M.; Pakula, T. *Polymer* **2002**, *43*, 5321–5328.
(28) Blais, J. J. B. P.; Geil, P. H. *J. Ultrastruct. Res.* **1968**, *22*, 303–311.
(29) Cohen, Y. *J. Polym. Sci., Part B: Polym. Phys.* **1996**, *34*, 57–64.
(30) Bertin, A.; Hermes, F.; Schlaad, H. *Adv. Polym. Sci.* **2010**, *224*, 167–195.
(31) Schatz, C.; Lecommandoux, S. *Macromol. Rapid Commun.* **2010**, *31*, 1664–1684.